BBA 68184

"HIT-AND-RUN" MECHANISM FOR D-GLUCURONATE REDUCTION CATALYZED BY D-MANNONATE:NAD OXIDOREDUCTASE OF *ESCHERICHIA COLI*

MARIE-ANDRÉE MANDRAND-BERTHELOT and ALAIN E. LAGARDE

Laboratoire de Microbiologie (406), Institut National des Sciences Appliquées de Lyon 69621 Villeurbanne CEDEX (France)

Summary

D-mannonate:NAD oxidoreductase (D-mannonate:NAD$^+$ 5-oxidoreductase, EC 1.1.1.57) from *Escherichia coli* normally catalyzes the reaction: D-fructuronate + NADH $\rightleftharpoons$ D-mannonate + NAD$^+$ [4,5]. It can also catalyze the reduction of D-glucuronate according to the equation: D-glucuronate + NADH $\rightarrow$ L-gulonate + NAD$^+$. Kinetic evidence is given for the second reaction to proceed in two steps: (i) NADH binds reversibly the free enzyme to form a binary complex E · NADH; (ii) D-glucuronate reacts subsequently with the binary complex to give products, without formation of an intermediary ternary complex E · NADH · glucuronate. The rate of the overall reaction obeys the classical Michaelis-Menten law with respect to NADH concentration ($K_1 = 0.03$ mM) but is proportional to D-glucuronate concentration in the range 0—100 mM.

Results concerning the action of several inhibitors on D-glucuronate reduction were interpreted satisfactorily by developing models based on mechanism involving an enzyme carrying one binding site for the alternative substrate D-mannonate and one binding site for the coenzyme NADH (Table I). In any case the experimental values of the dissociation constants for the complexes enzyme-effector were deduced. NAD and ATP act as strict competitive inhibitors ($K_2 = 0.60$ mM and 20 mM) able to bind the free enzyme only. In the case of ATP, a second binding site with a high affinity ($K_3 = 0.20$ mM) is unmasked when the first binding site is saturated. Mannonate and altronate behave as strictly noncompetitive inhibitors able to bind equally the free enzyme and the binary complex E · NADH. L-Gulonate acts as a mixed non-competitive inhibitor able to bind much easily the free enzyme ($K_4 = 0.41$ mM) than the complex E · NADH ($K_2 = 131$ mM). In no case was D-glucuronate shown to be able to react with complexes other than E · NADH. Such an unusual mechanism for a two-substrate enzyme looks similar to the sequence found by Chance for horseradish peroxidase [6].

Introduction

In *Escherichia coli*, the first step in the degradation of D-glucuronate is an isomerization catalyzed by D-glucuronate-ketol isomerase (EC 5.3.1.12) converting D-glucuronate into D-fructuronate [1,2]. We have isolated mutants of *E. coli* which are lacking in the uronic isomerase but were still found able to grow on D-glucuronate as the sole source of carbon and energy [2,3]. We gave evidence reported elsewhere [3] that the subsequent enzyme in the pathway, D-mannonate:NAD oxidoreductase (D-mannonate: NAD$^+$ 5-oxidoreductase, EC 1.1.1.57), responsible for the reduction of D-fructuronate into D-mannonate according to the reaction:

$$\text{D-fructuronate} + \text{NADH} + \text{H}^+ \rightleftharpoons \text{D-mannonate} + \text{NAD}^+ \qquad (1)$$

is able to reduce D-glucuronate into (most probably) L-gulonate according to:

$$\text{D-glucuronate} + \text{NADH} + \text{H}^+ \rightarrow \text{L-gulonate} + \text{NAD}^+ \qquad (2)$$
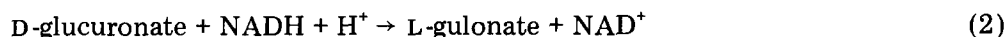
In this study we will assume that the reaction product is L-gulonate though its identity has not been firmly established yet [3].

D-mannonate:NAD oxidoreductase was partly purified by Portalier and Stoeber [4] and was shown to be a two-substrate enzyme obeying a "rapid-equilibrium random BiBi with dead-end EBQ complex" mechanism, according to the nomenclature of Cleland [5]. In contrast, experimental results presented in this paper indicate that the reduction of D-glucuronate catalyzed by D-mannonate:NAD oxidoreductase follows a completely different and unusual mechanism. Kinetics performed in the presence of several inhibitors support a model where D-glucuronate is reduced by the binary complex enzyme · NADH without formation of an intermediary ternary complex enzyme · NADH · D-glucuronate. This type of reaction is to be compared to the mechanism of horseradish peroxidase described in 1943 by Chance [6].

Materials and Methods

Bacterial strain. The source of enzyme was the strain GRS84, a derivative of the strain AU128 of *E. coli* K-12 [2,3]. It carries a mutation in the structural gene coding for the uronic isomerase ($uxaC^-$) [7] and requires thiamine and methionine for growth.

Enzyme preparation. Bacteria were grown in a minimum medium containing glycerol (4 mg/ml), L-methionine (100 μg/ml), thiamine hydrochloride (0.5 μg/ml) and D-glucuronate (4 mg/ml) as an inducer for D-mannonate:NAD oxidoreductase, as described previously [3]. Crude enzymatic fractions or Sephadex G-200 chromatography eluted fractions (purification factor: 25) were prepared according to the procedure detailed elsewhere [3]. Residual isomerase activity was found negligible in either fraction. Protein concentration was estimated according to the method of Lowry et al. [10] with bovine serum albumin as a standard.

Enzyme assay. The decrease of the NADH absorbance at 340 nm was followed upon addition of the enzyme preparation at a suitable dilution into a standard reaction medium similar to that used by Portalier and Stoeber [4] and

containing in a 1 ml final volume: sodium phosphate buffer, pH 6.3 (50 mM), NADH (0.20 mM), potassium D-glucuronate (50 mM) and other components as indicated for each experiment. The final protein concentration was 20—40 μg per ml for crude extracts and 0.5 μg per ml for purified fractions. Temperature was equilibrated at 30°C. A double beam spectrophotometer coupled to a recorder (Unicam SP1805) was used to monitor absorbance changes at 340 nm. Non-specific NADH oxidation was automatically corrected with a reference cuvette containing the reaction medium without D-glucuronate. Absorbance changes were linear for 2—3 min and initial rates were proportional to the amount of added enzyme under the above-mentioned conditions. One unit of enzyme activity (U) is defined as the amount of enzyme catalyzing the oxidation of 1 μmol NADH per min in the standard conditions described above. Rates are expressed in U per ml of reaction medium.

Chemicals. D-altronate, potassium salt, was synthesized according to the method of Pratt and Richtmeyer [8,9]. NADH and NAD$^+$ were obtained from Boehringer France and ATP from Schwartz Bioresearch. D-glucuronic acid was purchased from Sigma and L-gulono-γ-lactone from Fluka. Lactones were neutralized with KOH to pH 7.2. Other reagents were of the highest purity commercially available.

Results and Discussion

1. D-glucuronate reduction in the absence of effector

By drawing Lineweaver-Burk plots the initial rates of D-glucuronate reduction catalyzed by D-mannonate:NAD oxidoreductase, for a given concentration of substrate (D-glucuronate) and for varying concentrations of coenzyme (NADH), straight lines were obtained (Fig. 1). The K_m for NADH (K_m = 0.030 ± 0.003 mM) is identical to the value found previously by Portalier and Stoeber [4] when measuring the reduction of D-fructuronate. In addition we observed
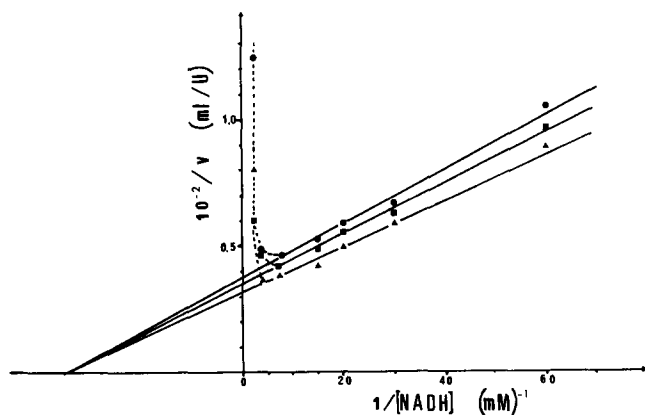

Fig. 1. Initial rate of D-glucuronate reduction as a function of NADH concentration. Lineweaver-Burk plots are given for the following D-glucuronate concentrations: ●, 40 mM; ■, 50 mM; ▲, 60 mM. The standard reaction medium described in Materials and Methods contained 20 μg protein of crude extract per ml.

an inhibition of enzymatic activity for high NADH concentrations, beyond 0.25 mM. The same K_m value for NADH was obtained whether using crude or purified enzyme preparations. In contrast, for a saturating concentration of NADH (0.20 mM) initial rates of D-glucuronate reduction were linearily dependent upon the D-glucuronate concentration in the range 0—100 mM (Fig. 2). These results were reproduced several times using crude or purified extracts and were taken to indicate that D-mannonate:NAD oxidoreductase by itself apparently exhibits no affinity for D-glucuronate. The unusual kinetic behaviour of D-glucuronate reduction catalyzed by D-mannonate:NAD oxidoreductase led us to investigate two-substrate enzyme models described in the literature. Horseradish peroxidase was found by Chance in 1943 [16] to form a binary complex with hydrogen peroxide which subsequently decomposes to give products in the presence of an oxygen acceptor such as ascorbate. Indeed, initial rates obeyed the Michaelis-Menten law with respect to hydrogen peroxide concentration but a linear law with respect to the acceptor concentration. Therefore, by analogy with the mechanism of the peroxidase, we proposed the model depicted in Fig. 3 for the mechanism leading to D-glucuronate reduction. The coenzyme NADH binds reversibly the free enzyme to form a binary complex E · NADH and a bimolecular reaction between this complex and the substrate (D-glucuronate) gives the products. The pecularity of this enzyme model is that no ternary complex E · NADH · D-glucuronate is involved. For the sake of simplicity, we assumed the occurrence of a unique binary complex.

If we make the assumption that the second step is rate-limiting in the sequence, the overall reaction velocity is given by:

$$v = k \cdot [E \cdot NADH][Glucuronate] \tag{3}$$

Square brackets indicate concentrations. When the steady-state theory of Briggs and Haldane [12] is applied to the model depicted in Fig. 3, the following rate
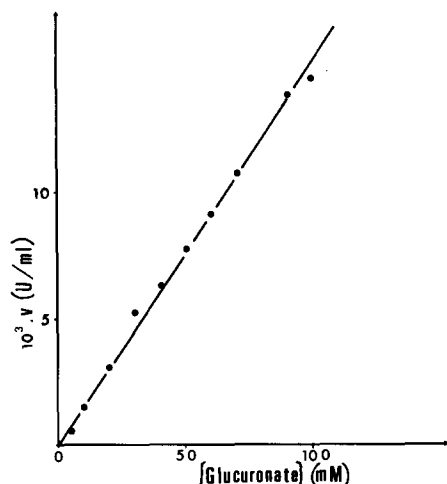

Fig. 2. Initial rate of D-glucuronate reduction as a function of D-glucuronate concentration. The standard reaction medium described in Materials and Methods contained a saturating NADH concentration (0.32 mM) and 20 μg protein of crude extract per ml.

$$\text{E} \quad + \quad \text{NADH} \quad \underset{k_{-1}}{\overset{k_{+1}}{\rightleftharpoons}} \quad \text{E-NADH} \quad \xrightarrow{k} \quad \text{E} \quad + \quad \text{NAD} \quad + \quad \text{L-Gulonate}$$
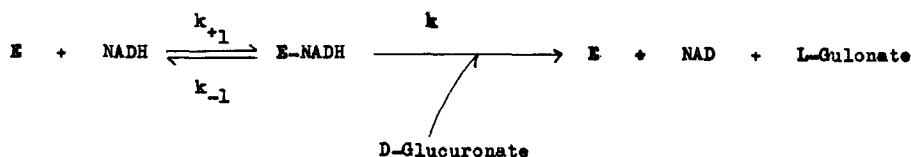
D-Glucuronate

Fig. 3. Kinetic model proposed for the D-glucuronate reduction catalyzed by D-mannonate:NAD oxido-reductase. Symbols: E, free enzyme; NADH, NAD, reduced and oxidized coenzymes; k_{+1}, k_{-1}, k, rate constants.

expression results:

$$v = \frac{k\,[\text{E}_\text{T}]\,[\text{NADH}]\,[\text{Glucuronate}]}{K_\text{m} + [\text{NADH}]} \tag{4}$$

where $[\text{E}_\text{T}]$ represents the total enzyme concentration and K_m, given by:

$$K_\text{m} = \frac{k_{-1} + k \cdot [\text{Glucuronate}]}{k_{+1}} \tag{5}$$

represents the Michaelis constant for NADH.

Results presented in Fig. 1 indicated that the K_m for NADH does not change appreciably with the concentration of D-glucuronate, so that the term: $k \cdot$ [Glucuronate] is negligible compared to k_{-1} and the K_m is given by:

$$K_\text{m} = \frac{k_{-1}}{k_{+1}} = K_\text{NADH} \tag{6}$$

K_NADH is the dissociation constant for the complex E $\cdot$ NADH. Eqn. 4 predicts that the rate is a saturable function of NADH concentration and a linear function of D-glucuronate concentration, in agreement with the results obtained in Figs. 1 and 2. The maximum rate of the reaction, $V = k \cdot [\text{E}_\text{T}]$ is given by the slope of the line $v = f$ ([glucuronate]), for a saturating NADH concentration. V is 0.008 U/mg protein with the crude extract (Fig. 2) and 0.50 U/mg protein with the purified enzyme fraction (not shown).

2. D-glucuronate reduction in the presence of effectors

2.1. Theoretical considerations. One methodological approach to test the plausibility of the mechanism involved in D-glucuronate reduction (Fig. 3) is to measure the activity in the presence of known inhibitors of D-mannonate: NAD oxidoreductase. We took advantage of the fact that NAD^+, ATP, mannonate and altronate inhibit D-fructuronate-catalyzed reduction as demonstrated by Portalier [5]. In order to facilitate the interpretation of our results, a number of kinetic models were devised starting from the assumption that an effector molecule could bind the free enzyme (E), the binary complex (E $\cdot$ NADH) or both (see Fig. 3). For the different cases under study, a classical steady-state treatment enabled us to derive the incomplete rate equation and then pertinent graphical representations (Lineweaver and Burk, Dixon, variation of K_m and maximal rate V with NADH or inhibitor concentration). This treatment led us to discriminate easily the eight models shown in Table I. The interesting consequence is that the dissociation constants of the various enzyme-effector complexes can be deduced in most cases.

TABLE I

k_{+n}, k_{-n}: forward and backward rate constants of step n, with n = 1, 2, 3 or 4. k, k': rate constants of D-glucuronate reaction with the enzyme · NADH complexes in absence and in presence of inhibitor respectively.
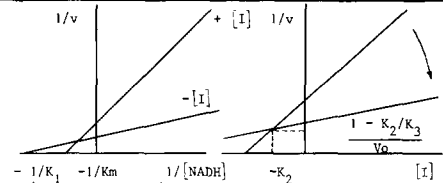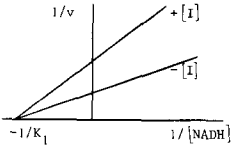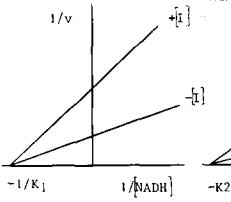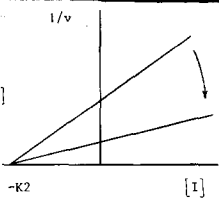
$$K_n = k_{-n}/k_{+n}$$

E: free enzyme. NADH, NAD: reduced and oxidized states of nicotinamide-adenin-dinucleotide. I: inhibitor. GLU: D-glucuronate, P: product of D-glucuronate reduction. [ ] indicates concentration. v, V: initial and maximal velocities. V_o: maximal velocity in absence of inhibitor. K_m: apparent Michaelis constant for NADH. *: in Dixon plots, the direction of the arrow indicates increasing concentrations of NADH.

Inhibition types

Case IA : mixed competitive-non competitive inhibition (hyberbolic)

$$E \underset{k_{-1}}{\overset{k_{+1} \text{ (NADH)}}{\rightleftharpoons}} E\text{-NADH} \overset{k \text{ (GLU)}}{\longrightarrow} NAD + P$$

$k_{+2}(I)$ ↕ k_{-2} k_{-3} ↕ $k_{+3}(I)$

k_{-4}

$$E\text{-I} \underset{k_{+4} \text{ (NADH)}}{\overset{}{\rightleftharpoons}} E\text{-I-NADH} \overset{k' \text{ (GLU)}}{\longrightarrow} NAD + P$$

$K_1 \neq K_2 \neq K_3 \neq K_4$ $k = k'$

$K_1 \cdot K_4 = K_2 \cdot K_3$

Case IB : mixed competitive-non competitive inhibition (linear)

idem case IA   with k' = 0

Case IIA : partially non-competitive inhibition

idem case IA   with $K_1 = K_4$

$K_2 = K_3$

Case IIB : strictly non-competitive inhibition

idem case IA   with $K_1 = K_4$

$K_2 = K_3$

k' = 0

TABLE I continued

		ANALYSIS OF INHIBITION KINETICS BASED ON THE
Graphical representation		**Parameters of the rate**
Lineweaver and Burk	Dixon*	
$1/v = f\ (1/[\text{NADH}])$	$1/v = f\ ([\text{I}])$	apparent V

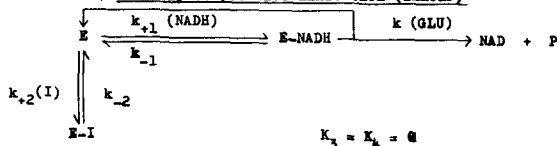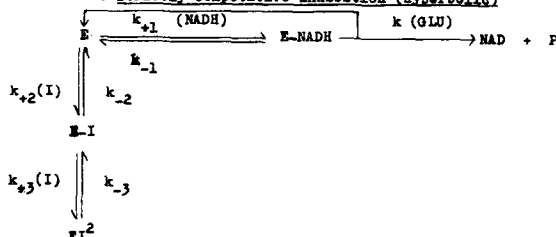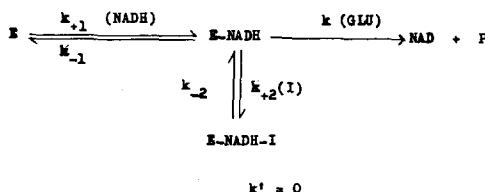| Lineweaver and Burk	Dixon	apparent V
non linear	non linear	$V_o \dfrac{1 + \dfrac{k'}{k} \cdot \dfrac{[\text{I}]}{K_2} \cdot \dfrac{K_1}{K_4}}{1 + \dfrac{[\text{I}]}{K_2} \cdot \dfrac{K_1}{K_4}}$
if $K_2 < K_3$ straight lines have a common intercept located in the upper left quadrant		$\dfrac{V_o}{1 + \dfrac{[\text{I}]}{K_2} \cdot \dfrac{K_1}{K_4}}$
	non linear	$V_o \dfrac{1 + \dfrac{k'}{k} \cdot \dfrac{[\text{I}]}{K_2}}{1 + \dfrac{[\text{I}]}{K_2}}$
		$\dfrac{V_o}{1 + \dfrac{[\text{I}]}{K_2}}$

REACTION MODEL DEPICTED IN FIG.3

equation : $v = \dfrac{V\,[\text{NADH}]}{Km + [\text{NADH}]}$

Criteria for identifying the inhibition case

apparent Km

|	
$K_1 \dfrac{1 + \dfrac{[I]}{K_2}}{1 + \dfrac{[I]}{K_2} \cdot \dfrac{K_1}{K_4}}$	- non linear graphical representations - V, decreasing hyperbolic function of $[I]$; tends towards k'/k when $[I] \longrightarrow +\infty$ - Km, decreasing hyperbolic function of $[I]$; tends towards K_4/K_1 when $[I] \longrightarrow +\infty$ - dissociation constants non deducible from Lineweaver-Burk and Dixon plots
$K_1 \dfrac{1 + \dfrac{[I]}{K_2}}{1 + \dfrac{[I]}{K_2} \cdot \dfrac{K_1}{K_4}}$	- linear graphical representations - V, decreasing hyperbolic function of $[I]$; tends towards 0 when $[I] \longrightarrow +\infty$ - Km, increasing hyperbolic function of $[I]$; tends towards K_4/K_1 when $[I] \longrightarrow +\infty$ - K_1 deduced from Lineweaver-Burk plots - K_2, K_3 and K_4 deduced from Dixon plots
K_1	- non linear Dixon plots - V, decreasing hyperbolic function of $[I]$; tends towards k'/k when $[I] \longrightarrow +\infty$ - $Km = K_1 = K_4$ (Lineweaver-Burk) - K_2 non deducible from Dixon plots
K_1	- linear graphical representations - V, decreasing hyperbolic function of $[I]$; tends towards 0 when $[I] \longrightarrow +\infty$ - $Km = K_1 = K_4$ (Lineweaver-Burk) - K_2 deduced from Dixon plots - $K_3 = K_2$

14

Case IIIA : <u>partially competitive inhibition</u>

idem case IA   with k = k'

Case IIIB : <u>strictly competitive inhibition (linear)</u>

$$E \xrightleftharpoons[k_{-1}]{k_{+1} \text{ (NADH)}} E\text{-NADH} \xrightarrow{k \text{ (GLU)}} NAD + P$$

$$k_{+2}(I) \Big\Updownarrow k_{-2}$$

$$E\text{-I} \qquad\qquad K_3 = K_4 = 0$$

Case IIIC : <u>strictly competitive inhibition (hyperbolic)</u>

$$E \xrightleftharpoons[k_{-1}]{k_{+1} \text{ (NADH)}} E\text{-NADH} \xrightarrow{k \text{ (GLU)}} NAD + P$$

$$k_{+2}(I) \Big\Updownarrow k_{-2}$$

$$E\text{-I}$$

$$k_{+3}(I) \Big\Updownarrow k_{-3}$$

$$EI^2$$

Case IV : <u>incompetitive inhibition</u>

$$E \xrightleftharpoons[k_{-1}]{k_{+1} \text{ (NADH)}} E\text{-NADH} \xrightarrow{k \text{ (GLU)}} NAD + P$$

$$k_{-2} \Big\Updownarrow k_{+2}(I)$$

$$E\text{-NADH-I}$$

$$k' = 0$$

2.2. Experimental results. All the assays were carried out at a fixed D-glucuronate concentration (50 mM) and varying concentrations of NADH and effector.

2.2.1. Inhibition by NADH analogues. Lineweaver and Burk plots obtained in the presence of either NAD^+ or ATP are linear and compatible with a competitive inhibition since $V = V_0$ and K_m is variable (Figs. 4A, 5A). However Dixon plots are linear in the case of NAD^+ (Fig. 4B) but hyperbolic in the case of ATP (Fig. 5B) as are the relationships between the Michaelis constant K_m and the concentration of effector (Figs. 4C, 5C).

When referring to Table I, NAD^+ inhibition would be consistent with the strict competitive type (Case IIIB) where the effector is able to bind the free
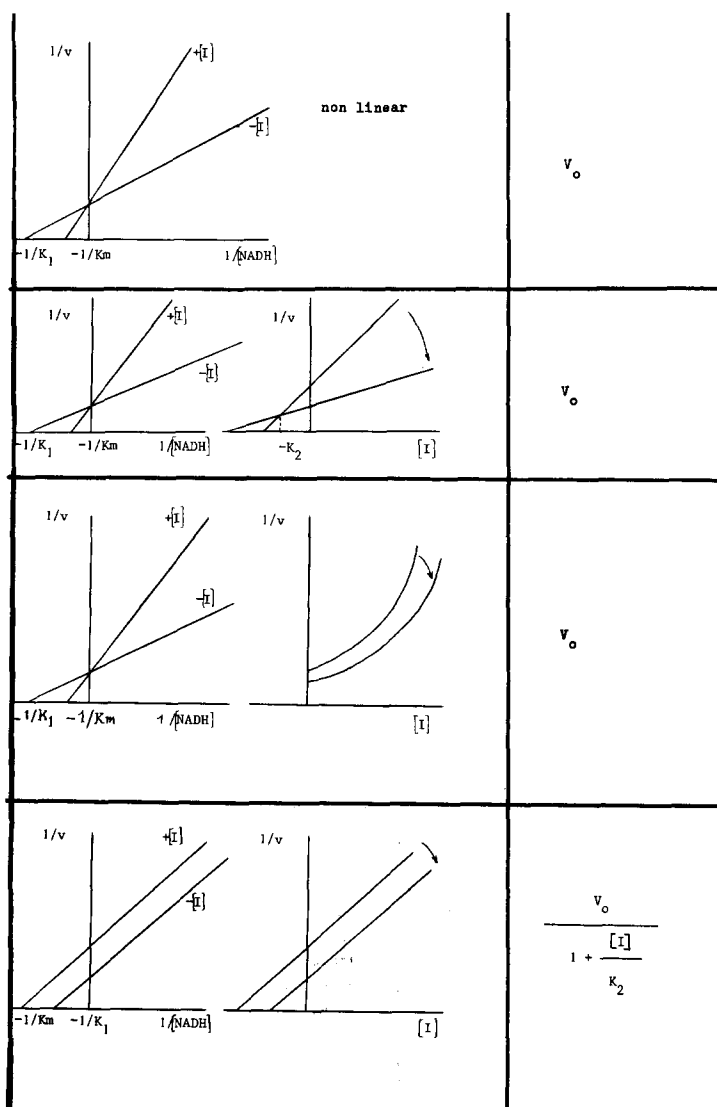
enzyme only. As shown in Table II the dissociation constant for the complex enzyme · NAD$^+$ (K_2 = 0.60 mM) is of the same order of magnitude as the value determined by Portalier (0.41 mM) [5] though slightly higher.

Results obtained with ATP are in agreement with hyperbolic strict competitive inhibition (Table I, case IIIC) where the free enzyme and the binary complex enzyme · ATP are able to bind one ATP molecule. Such a conclusion is strengthened by two further observations: (i) the K_m is a quadratic function of ATP concentration and obeys to following equation (Fig. 5D):

$$\frac{\dfrac{K_m}{K_1} - 1}{[\text{ATP}]} = \frac{1}{K_2} + \frac{1}{K_2 K_3}\,[\text{ATP}] \tag{7}$$

TABLE I continued

$$K_1 \dfrac{1 + \dfrac{[I]}{K_2}}{1 + \dfrac{[I]}{K_2} \cdot \dfrac{K_1}{K_4}}$$	- non linear Dixon plots - $V = V_o$ - K_m, increasing hyberbolic function of $[I]$; tends towards K_4/K_1 when $[I] \rightarrow +\infty$ - K_1 deduced from Lineweaver-Burk plots - K_2, K_3, K_4 non deducible from Dixon plots
$$K_1 \left[1 + \dfrac{[I]}{K_2} \right]$$	- linear graphical representations - $V = V_o$ - K_m, linear function of $[I]$ - K_1 deduced from Lineweaver-Burk plots - K_2 deduced from Dixon plots
$$K_1 \left[1 + \dfrac{[I]}{K_2} + \dfrac{[I]^2}{K_2 K_3} \right]$$	- hyperbolic Dixon plots - $V = V_o$ - K_m, quadratic function of $[I]$ - K_1 deduced from Lineweaver-Burk plots - K_2, K_3 deduced from : $$\dfrac{\dfrac{K_m}{K_1} - 1}{[I]} = \dfrac{1}{K_2} + \dfrac{1}{K_2 K_3} [I]$$
$$\dfrac{K_1}{1 + \dfrac{[I]}{K_2}}$$	- parallel straight lines in Lineweaver-Burk and Dixon plots - V_o, decreasing hyperbolic function of $[I]$; tends towards 0 when $[I] \rightarrow +\infty$ - K_m, decreasing hyperbolic function of $[I]$; tends towards 0 when $[I] \rightarrow +\infty$ - K_1 deduced from Lineweaver-Burk plots - K_2 deduced from Dixon plots (constant slope $= 1/K_2 . V_o$)

The dissociation constants of the three complexes as deduced from Fig. 5 are given in Table II. Since the dissociation constant of the ternary complex enzyme $\cdot$ (ATP)$_2$ is about two orders of magnitude smaller than the dissociation constant of the binary complex enzyme $\cdot$ ATP, one has to imagine that the binding of the first ATP molecule on the enzyme greatly enhanced the binding of the second ATP molecule; (ii) a strong positive cooperativity between the ATP binding sites on the enzyme molecule is indicated by Hill's plot (Fig. 5E) where the slopes of the straight lines obtained in the presence of different NADH concentrations are close to 2.
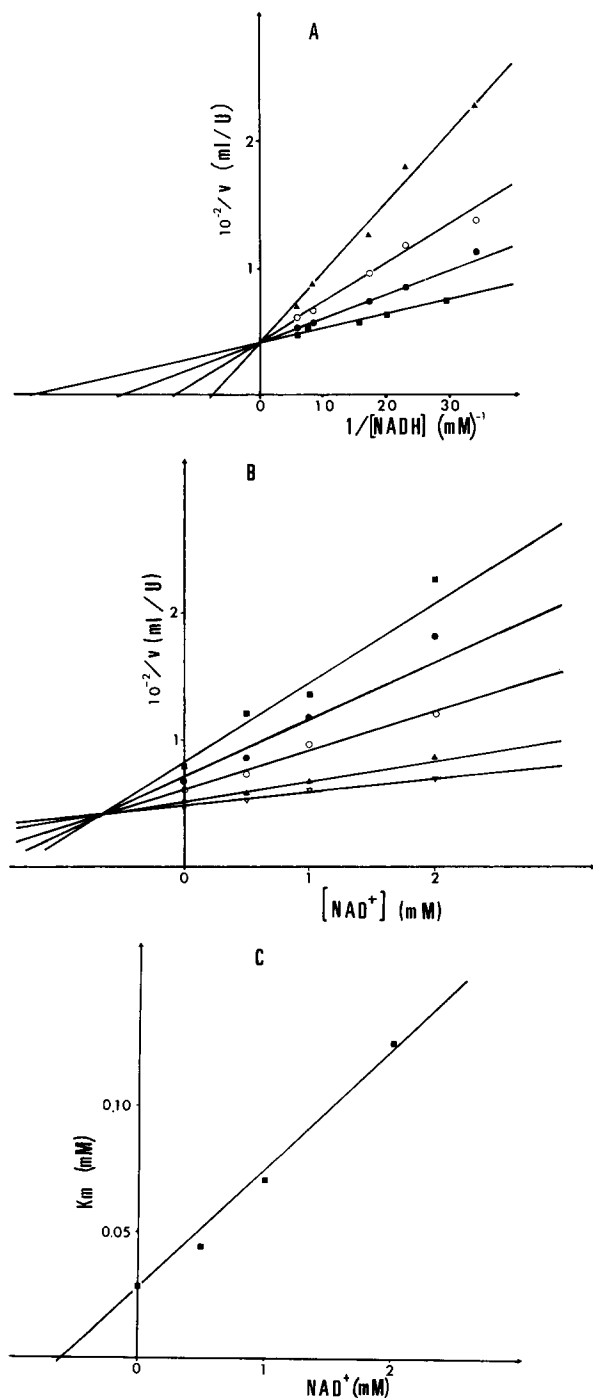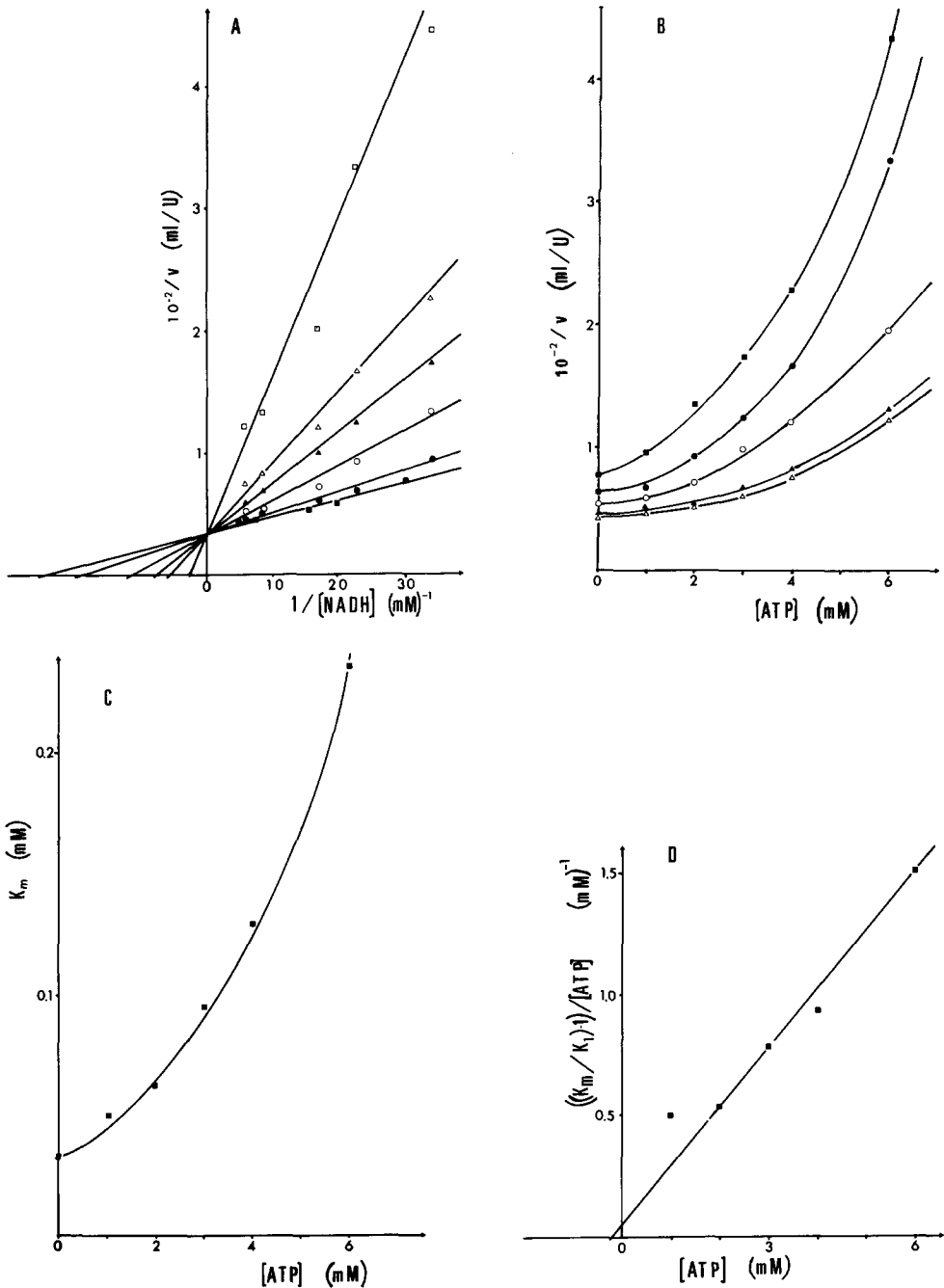
Fig. 4. Inhibition of D-glucuronate reduction by NAD. The standard reaction medium contained D-glucuronate (50 mM) and 40 μg protein of crude extract per ml. (A) Lineweaver-Burk plots. Variable substrate: NADH. NAD was present at the following concentrations: ■, none; ●, 0.5 mM; ○, 1 mM; ▲, 2 mM. (B) Dixon plots. NADH was present at the following concentrations: ■, 0.0292 mM; ●, 0.0438 mM; ○, 0.058 mM; ▲, 0.12 mM; ▽, 0.175 mM. (C) K_m variation as a function of NAD concentration. K_m values were deduced from the representation A.

2.2.2. Inhibition by D-mannonate and D-altronate. Lineweaver-Burk plots obtained in the presence of either mannonate (Fig. 6A) or altronate (Fig. 7A) are linear and have a common intercept on the abscissa axis in agreement with a non-competitive inhibition (Table I, case IIA or IIB). Dixon plots shown in
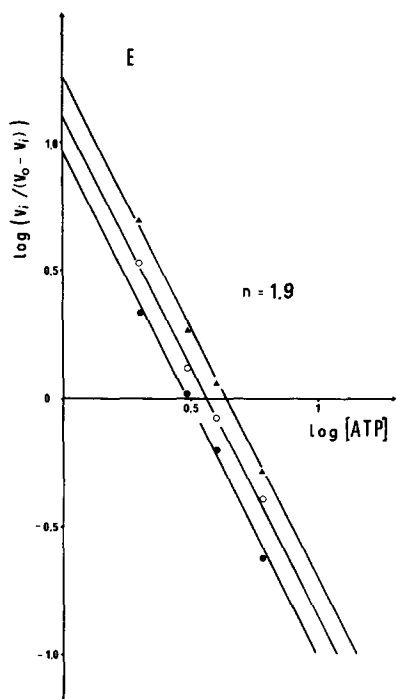
Fig. 5. Inhibition of D-glucuronate reduction by ATP. The standard reaction medium contained D-glucuronate (50 mM) and 40 μg protein of crude extract per ml. (A) Lineweaver-Burk plots. Variable substrate: NADH. ATP was present at the following concentrations: ■, none; ●, 1 mM; ○, 2 mM; ▲, 3 mM; △, 4 mM; □, 6 mM. (B) Dixon plots. NADH was present at the following concentrations: ■, 0.0292 mM ; ●, 0.0438 mM; ○, 0.058 mM; ▲, 0.12 mM; △, 0.175 mM. (C) K_m variation as a function of ATP concentration. K_m values were deduced from representation A. (D) Variation of $K_m/K_1-1/[ATP]$ versus ATP concentration (see Eqn. 7 in the text). (E) Hill plots : $\log v_i/(v_0-v_i) = f (\log [ATP])$ for the following NADH concentrations: ●, 0.0438 mM; ○, 0.058 mM; ▲, 0.12 mM. v_0 and v_i represent initial rates in the absence and presence of ATP respectively.
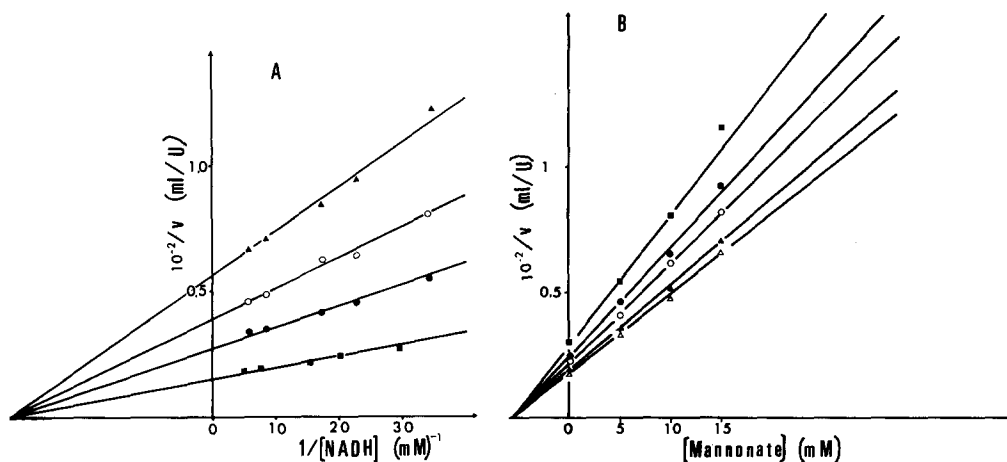

Fig. 6. Inhibition of D-glucuronate reduction by D-mannonate. The standard reaction medium contained D-glucuronate (50 mM) and 40 μg protein of crude extract per ml. (A) Lineweaver-Burk plots. Variable substrate: NADH. D-mannonate was present at the following concentrations: ■, none; ●, 5 mM; ○, 10 mM; ▲, 15 mM. (B) Dixon plots. NADH was present at the following concentrations: ■, 0.0292 mM; ●, 0.0438 mM; ○, 0.058 mM; ▲, 0.12 mM; △, 0.175 mM.

TABLE II

INHIBITION OF D-GLUCURONATE REDUCTION CATALYZED BY D-MANNONATE:NAD OXIDO-
REDUCTASE BY DIFFERENT EFFECTORS

Inhibitor *	Variable substrate	Inhibition type	Case	Dissociation constants of the enzyme-effector complexes (mM)			
				K_1^{**}	K_2^{***}	K_3^{***}	K_4^{****}
NAD	NADH	Strictly competitive (linear)	IIIB	0.028	0.60		
ATP	NADH	Strictly competitive (hyperbolic)	IIIC	0.033	20	0.2	
Mannonate	NADH	Strictly non-competitive (linear)	IIB	0.031	5.5	5.5	0.031
Altronate	NADH	Strictly non-competitive (linear)	IIB	0.029	5.2	5.2	0.029
Gulonate	NADH	Mixed non-competitive (linear)	IB	0.033	131	1640	0.41

* Varying concentrations of inhibitor were used for each experiment.

** K_1, dissociation constant of the enzyme · NADH complex, was deduced from Lineweaver-Burk plots.

*** K_2 and K_3 were deduced from Dixon plots except in the case of ATP where representation given in Fig. 5D was used.

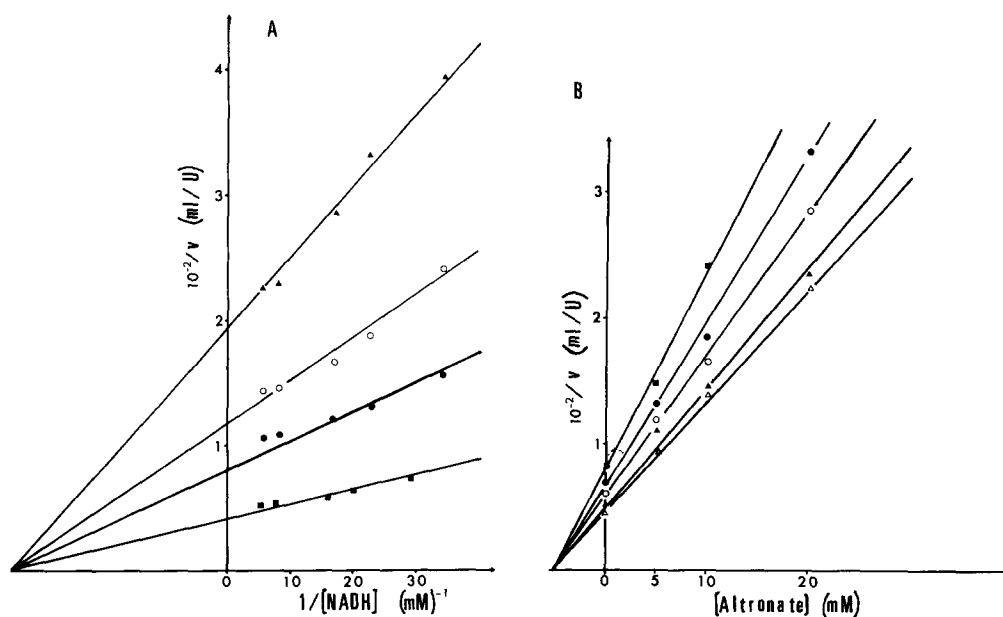**** K_4 was calculated from the relation imposed by thermodynamics: $K_1 \cdot K_3 = K_2 \cdot K_4$.

Fig. 7. Inhibition of D-glucuronate reduction by D-altronate. The standard reaction medium contained D-glucuronate (50 mM) and 40 μg protein of crude extract per ml. (A) Lineweaver-Burk plots. Variable substrate: NADH. D-altronate was present at the following concentrations: ■, none; ●, 5 mM; ○, 10 mM; ▲, 20 mM. (B) Dixon plots. NADH was present at the following concentrations: ■, 0.0292 mM; ●, 0.0438 mM; ○, 0.058 mM; ▲, 0.12 mM; △, 0.175 mM.

Fig. 6B and 7B are also linear and have a common intercept located on the abscissa axis, indicating that inhibition is strictly non-competitive (Table I, case IIB) and also that $K_2 = K_3$. Dissociation constants for the enzyme-effector complexes given in Table II are similar for mannonate and altronate suggesting that these two molecules bind equally well either the free enzyme or the enzyme · NADH complex. In agreement with the results obtained previously by Portalier [5] the binding of mannonate or altronate to the enzyme · NADH complex leads to a dead-end enzyme · NADH · effector complex.

2.2.3. *Inhibition by* L*-gulonate.* Since L-gulonate is the most likely product of D-glucuronate reduction catalyzed by D-mannonate:NAD oxidoreductase (see Eqn. 1) as reported elsewhere [3], we also analyzed L-gulonate as a possible inhibitor of D-glucuronate reduction. As shown in Fig. 8A, Lineweaver-
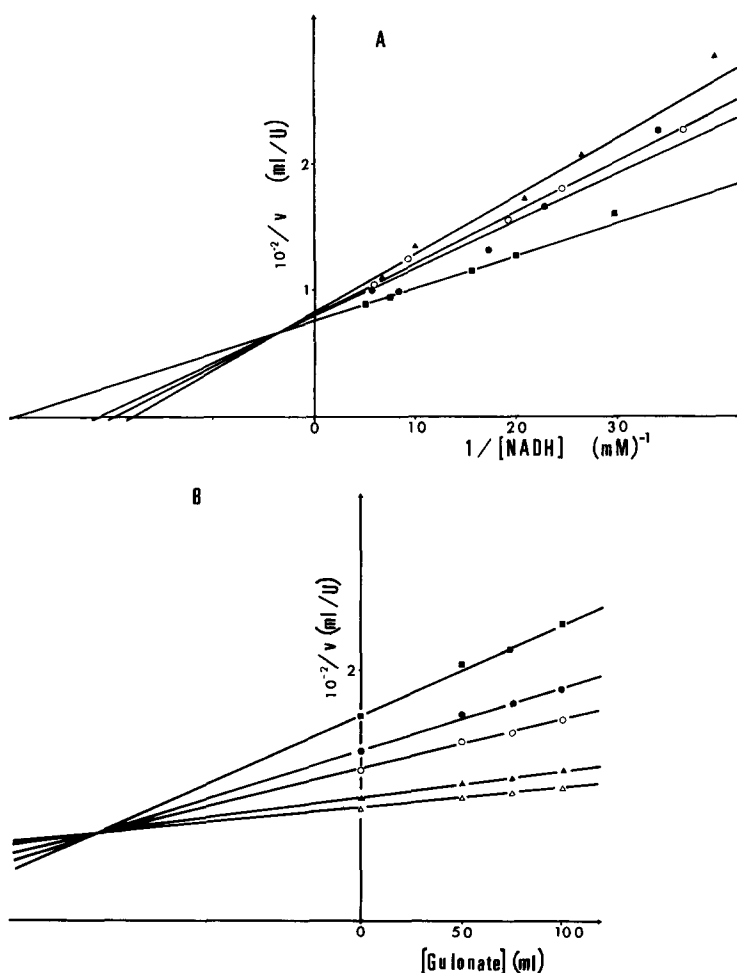

Fig. 8. Inhibition of D-glucuronate reduction by L-gulonate. The standard reaction medium contained D-glucuronate (50 mM) and 0.5 µg protein of purified enzyme per ml. (A) Lineweaver-Burk plots. Variable substrate: NADH. L-gulonate was present at the following concentrations: ■, none; ●, 50 mM; ○, 75 mM; ▲, 100 mM. (B) Dixon plots. NADH was present at the following concentrations: ■, 0.0292 mM; ●, 0.0438 mM; ○, 0.058 mM; ▲, 0.12 mM; △, 0.175 mM.

Burk plots are linear and have a common intercept located in the upper left quadrant, in agreement with a linear mixed competitive inhibition (Table I, case IB). Dixon plots are also linear (Fig. 8B) and have a common intercept located in the upper left quadrant, the abscissa ($-K_2$) corresponding to the dissociation constant of the enzyme-gulonate complex, the ordinate being equal to: $(1-K_2/K_3)/V_0$. The comparison of the dissociation constants for the four complexes involved (Table II) suggests that the affinity of D-mannonate:NAD oxidoreductase for L-gulonate is very low ($K_2 = 131$ mM) and also that reciprocal negative interaction occurs between the NADH- and L-gulonate-binding sites. Indeed when comparing K_1 with K_4 and K_2 with K_3, each binary complex (enzyme · NADH, enzyme · gulonate) appears to exhibit a reduced ability to bind another ligand compared to the corresponding ability of the free enzyme.

Conclusion

The experimental results taken as a whole bear out that the model proposed in Fig. 3 by analogy with the mechanism of horseradish peroxidase [6] is likely to hold for D-glucuronate reduction catalyzed by D-mannonate:NAD oxidoreductase. The analysis of several inhibitors of the enzyme based on models depicted in Table I are perfectly in agreement with known inhibitions occurring in the case of one-substrate enzymes. Therefore, the pecularity of D-glucuronate reduction consists in the fact that D-mannonate:NAD oxidoreductase behaves as a two-substrate enzyme when catalyzing D-fructuronate reduction [5] but as a one-substrate enzyme when catalyzing D-glucuronate reduction. The accurate mechanism taking place when the binary complex E · NADH reacts with D-glucuronate to give products cannot be known from the present work. However the finding that none ternary complex E · NADH · effector was able to react with D-glucuronate suggests that either some conformation of the complex E · NADH is required or that D-glucuronate needs to have access to a "binding site" on the enzyme molecule which is hindered by the binding of the effector. This "hit-and-run" mechanism [13] seems to be of widespread occurrence in the case of peroxidases and catalases [14] but was never described in the case of oxidoreductases. It would be of interest to use fast reaction techniques, as applied for instance to lactate dehydrogenase by Stinson and Gutfreund [15], in order to evaluate the rate constants k_{+1}, k_{-1} and k (Fig. 3) and elucidate the mechanism of D-glucuronate reduction.

The occurrence of two binding sites for NADH is inferred from the fact that high NADH concentrations lead to inhibition (Fig. 1) and also from the hyperbolic competitive inhibition caused by the analogue ATP (Fig. 5B, C). Interaction between binding sites located on the enzyme molecule are likely to occur (Fig. 5D, E) but the monomeric or polymeric nature of D-mannonate:NAD oxidoreductase remains to be assessed. The inhibition elicited by L-gulonate (Table II) is also consistent with the view that: (i) it may be the product of D-glucuronate reduction [3]; (ii) during D-glucuronate reduction, no ternary complex E · NADH · glucuronate is formed. L-gulonate was found previously to be slowly oxidized by D-mannonate:NAD oxidoreductase in the presence of NAD^+ [3].

Acknowledgements

References

1 Wahba, A., Hickman, J. and Ashwell, G. (1958) J. Am. Chem. Soc. 80, 2594—2594
2 Novel, G. and Stoeber, F. (1973) Biochimie 55, 1057—1070
3 Mandrand-Berthelot, M.A., Novel, G. and Stoeber, F. (1976) J. Bacteriol., submitted
4 Portalier, R. and Stoeber, F. (1972) Eur. J. Biochem. 26, 290—300
5 Portalier, R. (1972) Eur. J. Biochem. 30, 220—233
6 Chance, B. (1943) J. Biol. Chem. 151, 553—577
7 Portalier, R., Robert-Baudouy, J. and Nemoz, G. (1974) Mol. Gen. Genet. 128, 301—319
8 Pratt, J. and Richtmeyer, N. (1955) J. Am. Chem. Soc. 77, 1906—1908
9 Robert-Baudouy, J. (1971) 3e cycle Thesis, University of Lyon, Lyon
10 Lowry, O., Rosebrough, N., Farr, A. and Randall, R. (1951) J. Biol. Chem. 193, 265—275
11 Lineweaver, H. and Burk, D. (1934) J. Am. Chem. Soc. 56, 658—663
12 Briggs, G. and Haldane, J. (1925) Biochem. J. 19, 338—339
13 Reiner, J. (1964) in Comprehensive Biochemistry (Florkin, M. and Stotz, E.M., eds.), Vol. 12, pp. 126—164, Elsevier, Amsterdam
14 Brill, A. (1966) in Comprehensive Biochemistry (Florkin, M. and Stotz, E.M., eds.), Vol. 14, pp. 447—479, Elsevier Amsterdam
15 Stinson, R. and Gutfreund, H. (1971) Biochem. J. 121, 235—241